Influence of the chemical synthesis on the physicochemical properties of N-TiO2 nanoparticles

UNIVERSITÀ DEGLI STUDI DI TORINO

Influence of the chemical synthesis on the photocatalytic behaviour of N-TiO_2 nanoparticles for the degradation of microcystin-LR under visible light

S. Livraghi[1], M. Pelaez[3], J. Biedrzycki[1], I. Corazzari[1,2], E. Giamello[1], D. D. Dionysiou[3,4]

1 Dipartimento di Chimica, Università di Torino and NIS, Via P. Giuria 7, I - 10125 Torino, Italy

2 ''G. Scansetti'' Interdepartmental Centre for Studies on Asbestos and other Toxic Particulates

3 Environmental Engineering and Science Program, School of Energy, Environmental, Biological, and Medical Engineering, University of Cincinnati, Cincinnati, Ohio 45221-0012, USA

4 Nireas-International Water Research Centre, University of Cyprus, 20537 Nicosia, Cyprus

Abstract.

Nitrogen doped TiO_2 materials were successfully prepared following three different preparation routes (sol-gel, hydrothermal and pyrolysis) and characterized by various spectroscopic techniques. All samples absorbed radiation in the visible range and were active in the photocatalytic degradation of cyanotoxin microcystin-LR under visible light and in acidic conditions. The different preparation routes led to the formation of various impurities into the solids. In the case of hydrothermal and sol-gel samples, these impurities were weakly bound at the surface whereas the materials prepared by pyrolysis, the impurities showed a relevant stability and could not be removed even at high temperature. On the basis of the photocatalytic data illustrated in this paper, the presence of such species was not detrimental for the photocatalytic activity of nitrogen doped TiO_2 but actually contributed to a higher interaction with the target cyanotoxin; leading to a higher photocatalytic activity than that observed for samples prepared via the classic sol-gel method.

Introduction.

TiO_2 finds many applications in water and air purification using light (photocatalysis), however, it is well known that pure TiO_2 displays its peculiar photochemical and photophysical properties only under UV irradiation due to the high band gap value (3.2 eV for anatase polymorph) compatible only with the energy of UV photons. For this reason many efforts have been spent in the past to extend the photocatalytic performances of TiO_2 to the visible light in order to exploit more efficiently the solar light in all types of photocatalytic reactions [1].

Different strategies have been followed until now to reach this target such as doping with transition metal ions or surface sensitization with organic and organometallic dyes. More recently, doping TiO_2 with p-block (N, F, C, S) elements and in particular with nitrogen, has attracted the attention of the photocatalytic community as the introduction of such elements in the crystalline network produces materials capable of absorbing photons corresponding to visible radiation [2-5].

In previous work, research in our groups have shown that N doped TiO_2, known since 2001[6] to have some photocatalytic activity under visible light, when prepared by wet chemistry methods contains photoactive centres based on interstitial N atoms bound to lattice oxygen ions which are excited by photons of about 440 nm. These centres (labelled as $N_iO^{\bullet}$) are paramagnetic and were identified via Electron Paramagnetic Resonance (EPR) spectroscopy [7-9].

A significant number of papers on N doped titania have appeared in the past few years, mainly focused either on new photocatalytic results or on different approaches to unravel the nature of the bulk photoactive centres present in this system while a systematic study on the role of several other factors of vital importance for the photocatalytic process are still lacking. Among these factors we recall: i) the preparation procedure of the photocatalyst, ii) the nature of the impurities present in the material and iii) the state of the surface after preparation. In the present contribution we report results concerning different N doped TiO_2 materials prepared by three distinct wet chemistry methods (sol-gel synthesis, hydrothermal synthesis and pyrolysis) in order to investigate the relationships between the preparation procedure, the physicochemical properties of the materials and their photocatalytic properties.

All materials were first characterized to ensure the presence of N photoactive centres and, secondly, to identify the presence of other centers formed during preparation in order to understand their role on the promotion or inhibition of the photochemical phenomena. It is reported in the literature, in fact, that a high level of doping does not necessarily correspond to a high photocatalytic performance [10,11]. The dopant element, in fact, usually lead to active species for photocatalysis under visible light but, at the same time, it can form species having a detrimental effect on the material photoactivity [12].

Therefore, this variation of the chemical synthesis of N-TiO_2 can be directly related to the photocatalytic efficiency under visible light irradiation. The evaluation of these materials was performed in engineered water processes for the photocatalytic degradation of microcystin-LR (MC-LR); a widely found cyanotoxin in various water sources worldwide. Cyanotoxins are secondary metabolites with diverse chemical structure that are released from different genera of harmful cyanobacteria during bloom events. They are highly soluble in water, chemically stable and pose high toxicity (as hepatotoxicity, cytotoxicity or neurotoxicity) which represents a potential health risk to humans and the environment. MC-LR has been selected as target contaminant since it has been intensively investigated due to its continuous presence in higher concentrations than the provisional guideline for potable water proposed by the World Health Organization (1 μg/L), it has high toxicity, and it has been reported to cause health-related effects in humans and animals around the world. Previous work indicates that MC-LR can be subject to photocatalytic degradation with conventional and non-metal doped TiO_2 under UV and visible light [13-17].

2 Materials and Methods.

Three different methods for the preparation of N-doped TiO_2 were employed in this work. The first one was the classic sol gel synthesis (hereafter SG), via hydrolysis of titanium isopropoxide and NH_4F as nitrogen source, as described elsewhere [18]. The second method was the hydrothermal synthesis (HT) based on the treatment of a TiO_2 xerogel (typically 0.8 g) in the presence of 25 ml NH_3 for 5 days at 430K in a 125 ml hydrothermal reactor. The third material was synthesized via pyrolysis (PY) heating a mixture of Ti-isopropoxide, ethanol, urea and a 0.5M HCl solution (molar ratio 2:70:7:1 respectively) for 30 minutes in a furnace preheated at 573K. All materials after synthesis underwent a final calcination in air at 773K for 1 hr.

The structural characterisation was performed by X-ray diffraction (XRD) using a Philips 1830 diffractometer (K_α(Co) source) and a X'Peret High-Score software for data handling. Surface area was measured by a surface area analyzer (ASAP 2020, Micromeritics – USA). UV-Vis. diffuse reflectance (DR UV-Vis.) spectra were recorded by a Varian Cary 5/UV-Vis-N.I.R. spectrometer using a Cary win-UV scan software to follow the visible absorption enhancement due to nitrogen doping.

Electron Paramagnetic Resonance (EPR) spectra were run on a X-band CW-EPR Bruker EMX spectrometer operating at 100 KHz field modulation.

FTIR (Fourier Transform Infra-Red) spectra were obtained by a Brucker IFS 66 spectrophotometer equipped with an MCT cryogenic detector. The samples were inspected in the form of pellet in a

FTIR cell connected to a conventional high-vacuum apparatus (residual pressure < 10^{-3} Pa) which allowed a heat treatment of the samples.

An on-line Thermal Gravimetric Analysis coupled with Fourier Transform Infra-Red instrument (TGA–FTIR) from Perkin-Elmer (Waltham, MA, USA) was used to simultaneously analyze the weight loss of the powders and the nature of the molecules released by the samples upon heating.

For the TGA analysis the ultra-microbalance Pyris 1 from Perkin-Elmer (sensitivity 0.1 μg) was used. The materials were heated under O_2 flow (30 cm^3 min^{-1}) at a heating rate of 25K min^{-1} in the 298K - 1173K range. A relatively large amount of sample (ca. 20 mg) was heated in each run to optimize the amount of gases released. FTIR analysis of the evolved gas was carried out by a Spectrum 100 (Perkin-Elmer) spectrometer in the 600 cm^{-1}-4000 cm^{-1}.

The photocatalytic degradation of MC-LR was carried out in a batch system. The experiments were performed by adding a suspension of the nanoparticles (0.5 g/L), previously sonicated (2510R-DH, Bransonic), to an acidic solution (pH 3.0 ± 0.1) containing 600 ± 20 μg/L of MC-LR (Calbiochem). The photocatalytic reactor, a borosilicate glass Petri dish, was continuously mixed and irradiated under visible light (λ>420 nm) with two 15W fluorescent lamps equipped with a UV block filter (UV 420, Opticology). An average light intensity of 7.5 x 10^{-5} W cm^{-2} was measured with a broadband radiometer (Newport Corporation). The quantification of the samples, previously filtered (L815, Whatman) and taken at specific interval times, was performed by liquid chromatography (LC, Agilent Series 1100). Details of the analytical method can be found elsewhere [19].

3 Results and discussion

Table 1 summarizes the main properties (see S.I. also) of the three differently prepared N-TiO_2 materials.

Sample	Dopant	Composition % wt (Anatase)	Composition % wt (Rutile)	Surface Area (m^2/g)
HT	N	100	0	75
PY	N	90	10	48
SG	N + F	100	0	50

Table 1: Main properties of the three types of N-TiO_2 materials (dopants, phase compositions and surface areas).

3.1 EPR characterization.

N- TiO_2 was characterized by the presence of paramagnetic species whose EPR spectrum has been widely discussed in previous work [4,5,6]. The main paramagnetic species (indicated as $N_iO^{\bullet}$) was

present in all samples investigated (Fig. 1) and can be described in terms of interstitial nitrogen into the TiO_2 lattice. This species is the photoactive centre as proved on the basis of irradiation experiments showing that its EPR spectral intensity varies when irradiating the sample at a wavelength corresponding to the maximum of the optical absorption in the visible region [8].

Other nitrogen containing paramagnetic species observed in the materials here analyzed are NO (nitric oxide, present in the spectra of Fig. 1B and 1C) and NO_2 (nitrogen dioxide, traces in Fig. 1C) which are essentially by-products formed during the final calcination which do not influence the electronic structure of the solid.

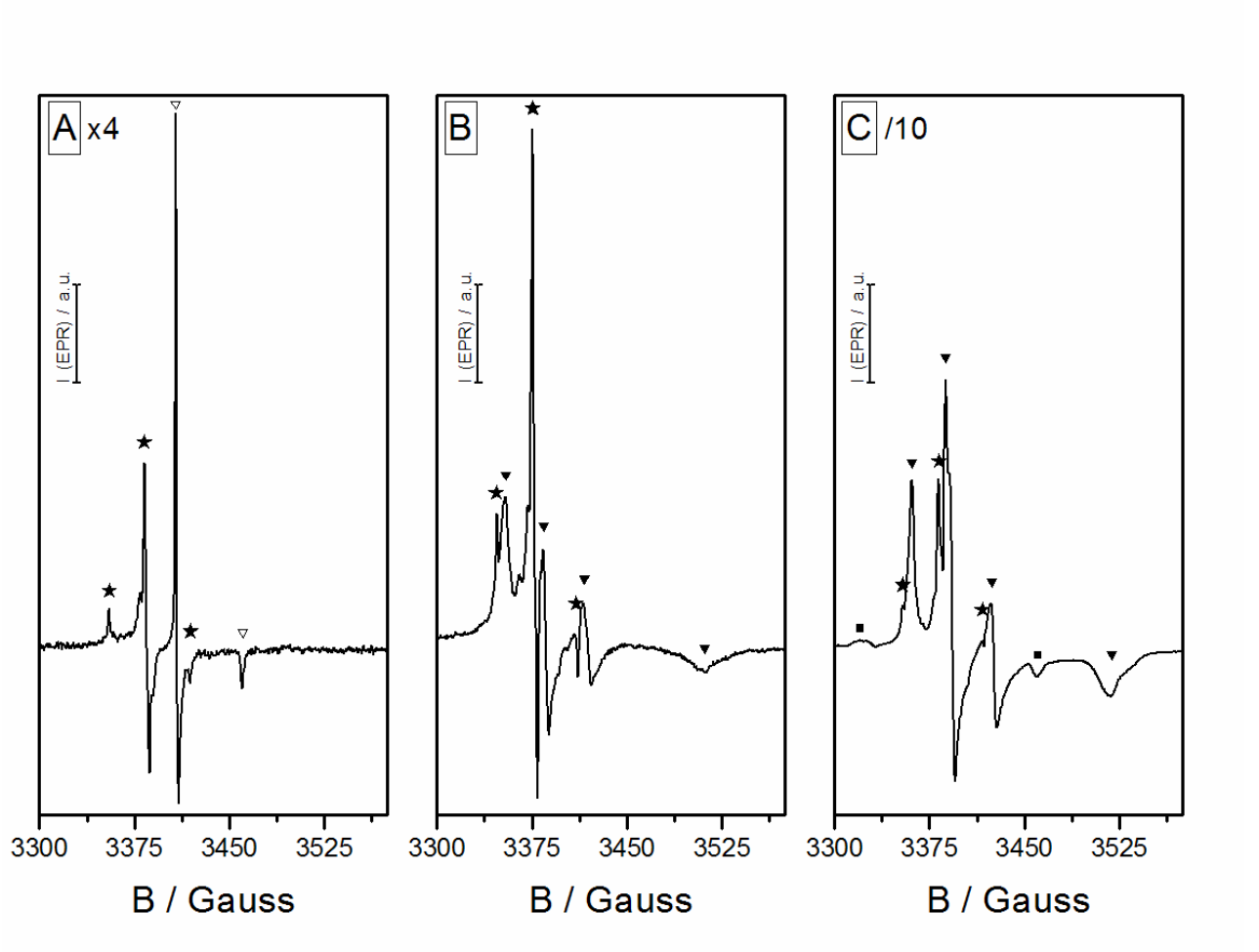

Figure 1: EPR spectra of differently prepared N-TiO_2 . A) SG sample. B) PY sample. C) HT sample.★ indicates $N_iO^{\bullet}$ species. ▼ indicates $NO^{\bullet}$ species, ▽ indicates Ti^{3+} species , ■ indicates NO_2 species.

Molecular $NO^{\bullet}$ and NO_2 are segregated in closed pores (or microvoids) within the crystals. Their EPR spectrum is not observable in the gaseous state but becomes visible at low temperature when the molecule is weakly adsorbed and polarized on a cationic centre at the inner surface of the cavity. Confinement of these gaseous molecules in the cavities is the reason why the two species are not removed by simple evacuation. [12,20].

In the case of the sample prepared via sol-gel (SG), beside the $N_iO^\bullet$ species, a second EPR signal is observed (Fig. 1 A). Its axial g tensor ($g_{\|}$=1.962 and $g_{\perp}$= 1.992) with both parallel and perpendicular components lower than 2.0023 (g_e) unambiguously indicates that the signal is due to Ti^{3+} ions in tetragonally distorted symmetry which are located in the bulk. The presence of Ti^{3+} in the solid is a direct consequence of the substitution of O by F in some lattice site of the structure. The extra electron introduced by F in the system is thus stabilized by Ti^{4+} ions [3]. The solid can thus be written with regard to the fluorine modification, in the following chemical terms: $Ti_{1-x}^{4+}Ti^{3+}{}_xO^{2-}{}_xF^-{}_x$

In summary, these results indicate that the photoactive N species observed by EPR ($N_iO^\bullet$) were present in all samples whatever the preparation adopted. Nitrogen oxides are also present in two of the samples, the gaseous molecules being confined in microvoids of the system without a serious influence on the properties of the system itself. In the case of SG materials the use of ammonium fluoride in the preparation caused F insertion in the lattice and consequently the formation of EPR visible Ti^{3+} ions (Fig. 1A) due to valence induction.

3.2 TGA-FTIR characterization.

The three materials investigated in the present work still contain, after calcination, a certain amount of surface impurities which are potentially capable of influencing the surface reactivity of the solid . In order to investigate this point and to compare the amount of contaminant present in the three samples, thermogravimetric analysis (TGA) was performed (Fig. 2). Beside physisorbed and chemisorbed water (due to the atmospheric contamination), nitrogen and carbon containing species are expected to be the main contaminants in all materials because of the chemical nature of the reactants used in the preparation. All TG measurements were carried out in oxygen flow in order to fully oxidize all chemical species. The three samples roughly exhibit the same weight loss (~3.5% wt, Fig. 2A-C) even though with a different profile of the various thermograms. The loss of weight for both PY and HT samples starts at low temperature and proceeds until c.a. 1073 K (Fig. 2A-B). In the case of the SG sample the weight loss at low temperature is less pronounced until c.a. 723 K. At this temperature a dramatic weight loss occurs as pointed out by the pronounced peak in the derivative curve, followed by a moderate weight loss similar to that observed for the other samples, and observed till 1073 K (Fig. 2C).

In the three cases no traces of NOx species were detected in the released gas indicating that the thermally decomposed nitrogen impurities are lower than the instrument detection limit and represent a negligible amount of the total surface species.

As to the content of carbon impurities, HT and PY samples have a very similar CO_2 emission profiles (Fig. 2A' and B'), except for a small emission at 873 K in the case of the PY material,

indicating the presence in this material only of a particularly stable carbon containing species in this material only. Water desorption is also quite similar for HT and PY samples being due (fast desorption in early stages of the experiment) to weakly adsorbed water molecules. In the case of SG prepared sample, the TGA profile is quite different with respect to that of the other samples (Fig. 2C and C'). This different behaviour can be ascribed to the presence, on the surface, of F^- groups replacing the OH^- groups. It has been reported in fact that the use of fluorine containing compound in the preparation of doped TiO_2 always leads not only to bulk doping but also to the simultaneous fluorination of the surface [3,21]. This fact is confirmed in the present case by XPS analysis (not reported for sake of brevity) showing the typical peaks of surface F^- ions. In this case (SG sample), CO_2 and H_2O desorption are basically absent (curves a and b in Fig. 2C') in agreement with experimental evidences of a lower affinity for water. More over at relatively high temperature (723K) other two different compounds are desorbed (profiles c and d in Fig. 2C'). By comparison with literature data the two species c and d can be tentatively assigned to fluorine containing species. Further work is needed to confirm this assignment.

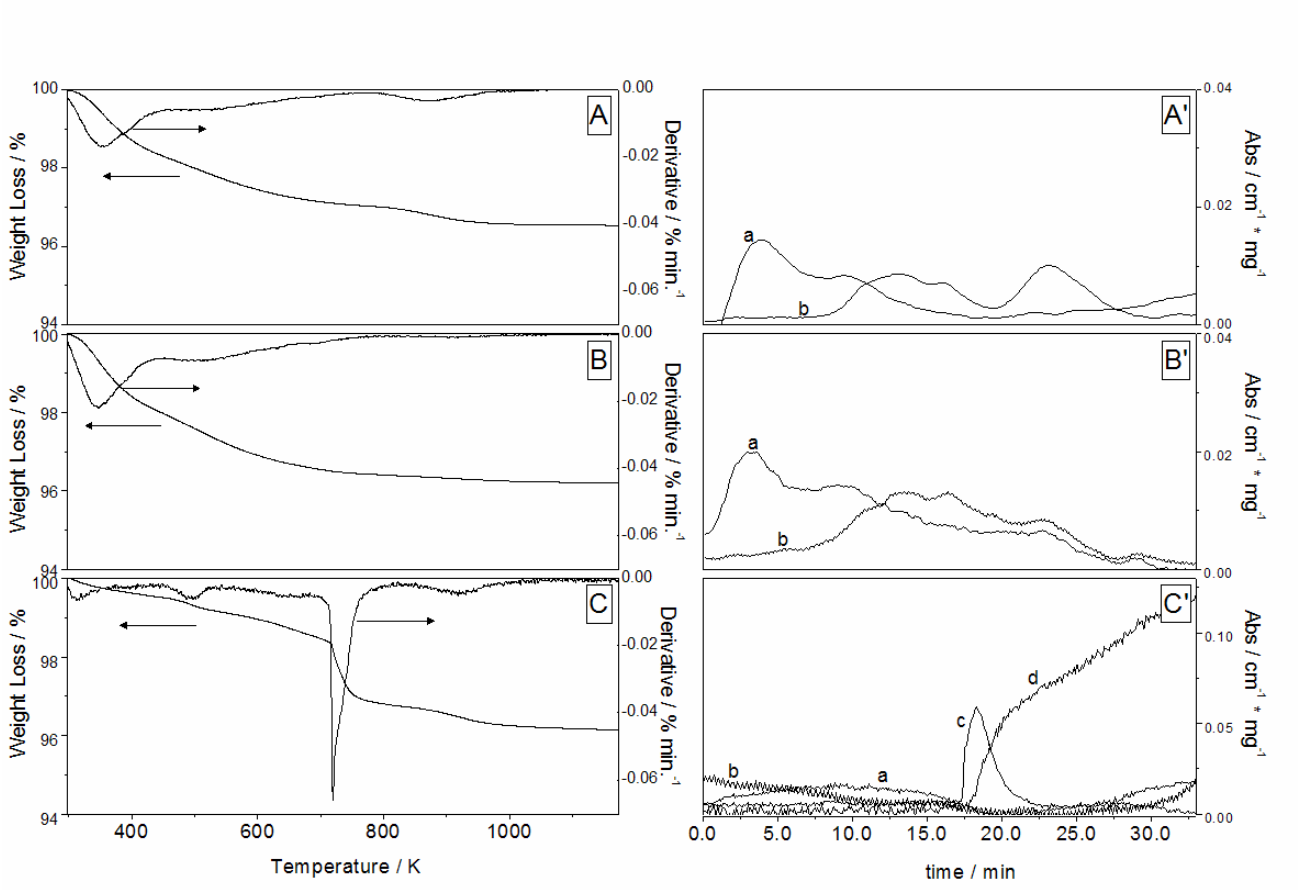

Figure 2: Thermogravimetric analysis of N-TiO_2. Left: percentage of weight loss and corresponding derivative; A) PY, B) HT, C) SG. Right: corresponding emissions of. H_2O, (a) CO_2 (b). Profiles labelled by c and d correspond to unidentified F species (see text)

3.3 FTIR characterization.

The nature of the various impurities present in the three materials has been investigated via FTIR spectroscopy. In Figure 3 the IR spectra of pristine calcined materials simply outgassed at room temperature (panel A) and after a mild thermal treatment under vacuum (T= 773K), performed in order to clean the surface from weakly bound species, (panel B) are reported. The spectral profile of the material prepared via pyrolysis appears, at first sight, much more complex than the others in terms of number and type of chemical impurities present in the solid.

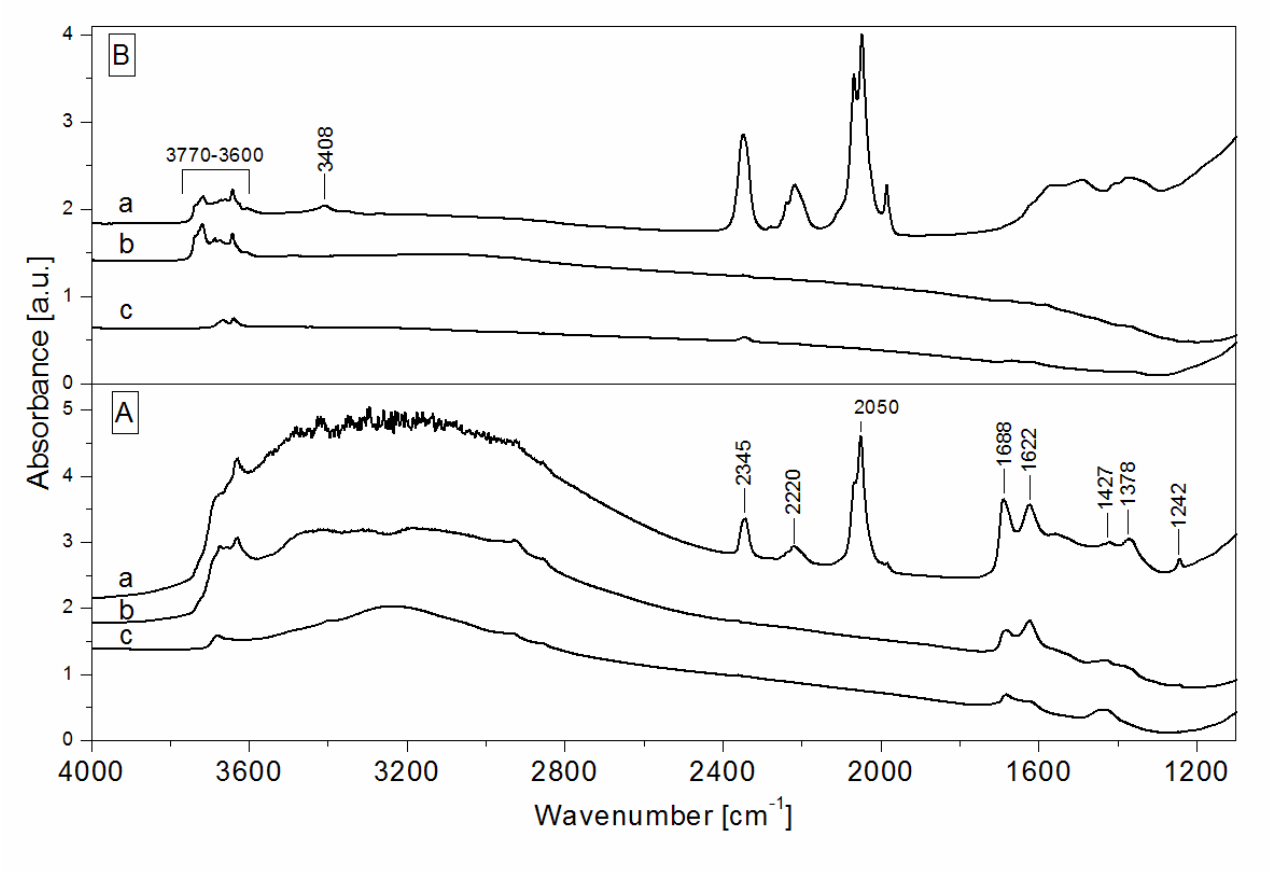

Figure 3: IR spectra of N-TiO_2 prepared via pyrolysis (a), hydrothermal (b) and sol-gel (c) synthesis outgassed at room temperature (A) and 1h at 500°C followed by reoxidation (B).

3.3.1 IR Spectra of Materials Outgassed at Room Temperature.

FTIR spectra of all samples outgassed at room temperature (Fig. 3 panel A) have some common features, and namely: i) a series of quite narrow peaks between 3770-3600 cm^{-1}; and at 2900 cm^{-1} due to isolated surface OH groups and aliphatic C-H groups respectively; ii) a broad absorption between 3800-2800 cm^{-1} due to interacting surface OH groups and to physisorbed water; iii) a further complex set of absorption bands at low wavenumbers between 1750 cm^{-1} and 1200cm^{-1}. The

peak at ca. 1620 cm^{-1} (due to adsorbed water molecules) has lower intensity in the case of the SG sample in agreement with the TGA data. The reduced water desorption is an effect of surface fluorination which limits the presence of surface hydroxyl groups. The other features at lower frequencies (1620 cm^{-1}, 1370 cm^{-1}, 1690 cm^{-1}) are ascribed to carbonate-like and bidentate carbonates, respectively [21-24].

In the case of PY sample (Fig. 3, panel A, trace a) other three main signals at 2345 cm^{-1}, 2220 cm^{-1} and 2050 cm^{-1} were observed. A CO_2 vibrational mode, typically split in two components due to the rotovibrational contour, is usually observed at 2340 cm^{-1}. In the present case, the unresolved peak at 2345 cm^{-1} is ascribed to linear CO_2 trapped into the microvoids of the TiO_2 particles. This finding is parallel to the observation of $NO^{\bullet}$ molecules also trapped within the pores (see section 3.1) and is consistent also with previous IR and Raman work [25]. The presence of molecular CO_2 is due to the oxidation of the precursor employed during the synthesis.

The spectral region between 2200-1900 cm^{-1} is typical of vibrations due to species characterized by double and triple bond between carbon and nitrogen. The presence of such compounds is the consequence of the use of urea as nitrogen source in the synthesis. It has been already reported that urea decomposition leads to several products like isocianate (-CNO), biuret (NH_2-CO-NH-CO-NH_2) and other compounds, or to heterocyclic compounds as melamine and its derivates [26,27]. For example, D. Mitoraj et al. showed that employing urea in the synthesis of N-TiO_2, melamine can be formed and polycondensation of this compound can occur with formation of coloured oligomers also responsible for visible light absorption of TiO_2 [28,29].

On the basis of literature data, the band at c.a. 2220 cm^{-1} observed in the present work is assigned to isocyanate group [30-32]. The assignment of the peak at c.a. 2050cm^{-1} is not totally unambiguous, even though an attribution to diazo-like compounds (-CNN-) seems very likely on the basis of the vibrational frequencies of such entities which are compatible with that observed here [33].

3.3.2 IR Spectra of Materials Outgassed at high Temperature.

In order to discriminate between impurities located in the bulk or at the surface of the solids, FTIR spectra were also recorded after outgassing the various N-TiO_2 materials at high temperature (Fig. 3 panel B) in order to decompose and remove the majority of surface contaminants.

In the cases of SG and HT samples, except for the peaks associated to residual isolated surface OH groups which are very resistant to outgassing, all main IR signals disappear indicating that the corresponding species are easily removed. Also in the case of PY sample, the broad absorption between 3800cm^{-1} and 2500cm^{-1} vanished upon high temperature outgassing revealing, like in the other two cases, the features of isolated OH groups and of a weak band at c.a. 3400cm^{-1} due to

residual ammonium ions. The latter band is not observed in panel A (RT desorption) because the N-H vibration mode is buried in the complex pattern of OH vibrations. In contrast to the behaviour of the other two samples, the material obtained via pyrolysis (PY) shows components (frequency between 2200-1900 cm^{-1} and 1750-1200cm^{-1}) which persist after the high temperature treatment corresponding to stable species. The peak intensity corresponding to C and N based compounds also increases indicating, in agreement with TGA data, that a chemical evolution of the system continues after calcination.

3.4 Photocatalytic evaluation.

The photocatalytic activity of the SG, HT and PY-prepared N-TiO_2 under visible light was examined via the photocatalytic degradation of MC-LR in aqueous solution at pH 3.0. Firstly, the amount of adsorbed MC-LR into each photocatalyst was determined under dark conditions in order to differentiate from visible light-activated photocatalysis. Figure 4A shows the extent of adsorption onto the different N-TiO_2 samples. Similar adsorption capacities were observed for N-TiO_2 with SG and HT and a slightly higher adsorption of MC-LR with N-TiO_2 from PY was observed. Interestingly, the material with the highest surface area (HT) exhibited the lowest adsorption capacity. This indicates that not only the surface area is an important parameter to consider during adsorption but the more complex surface of the sample prepared via pyrolysis (see section 3.3) contributed to a higher adsorption of MC-LR under acidic conditions. The functionality at the surface of PY sample can bind better to MC-LR than hydroxyl groups found in the other two samples. Moreover, the presence of F ions in the SG sample can contribute to a higher hydrophobicity of the material and decrease surface interaction between the photocatalyst and the cyanotoxin at the conditions tested.

When the samples were irradiated with visible light, all N-TiO_2 samples exhibited visible light-photoactivation as higher MC-LR removal was achieved compared to dark conditions. Degradation of MC-LR is negligible when pure TiO_2 is irradiated by visible light [14,16]. This confirmed the presence of the photoactive N containing species that are responsible for the photoactivation of N-TiO_2 and the formation of reactive oxygen species under visible light. HT and PY-prepared nanoparticles showed higher degradation of MC-LR compared to SG at an initial loading concentration of 0.5 g/L (Fig.4A). The effect of initial N-TiO_2 loading in solution was investigated and the results are shown in Figure 4B. Higher degradation of MC-LR was achieved by increasing the initial N-TiO_2 loading to 1g/L; regardless of the synthesis procedure employed for each sample. However, complete degradation was observed with HT and PY-prepared samples after 3 hr of visible light irradiation. The higher photocatalytic activity with HT and PY is in agreement with the

previous observation at a lower loading. The obtained results indicate that by increasing the initial concentration, the effectiveness on the removal of the cyanotoxin increased and complete degradation can be obtained without having light scattering and reduction of light penetration at the 1 g/L loading.

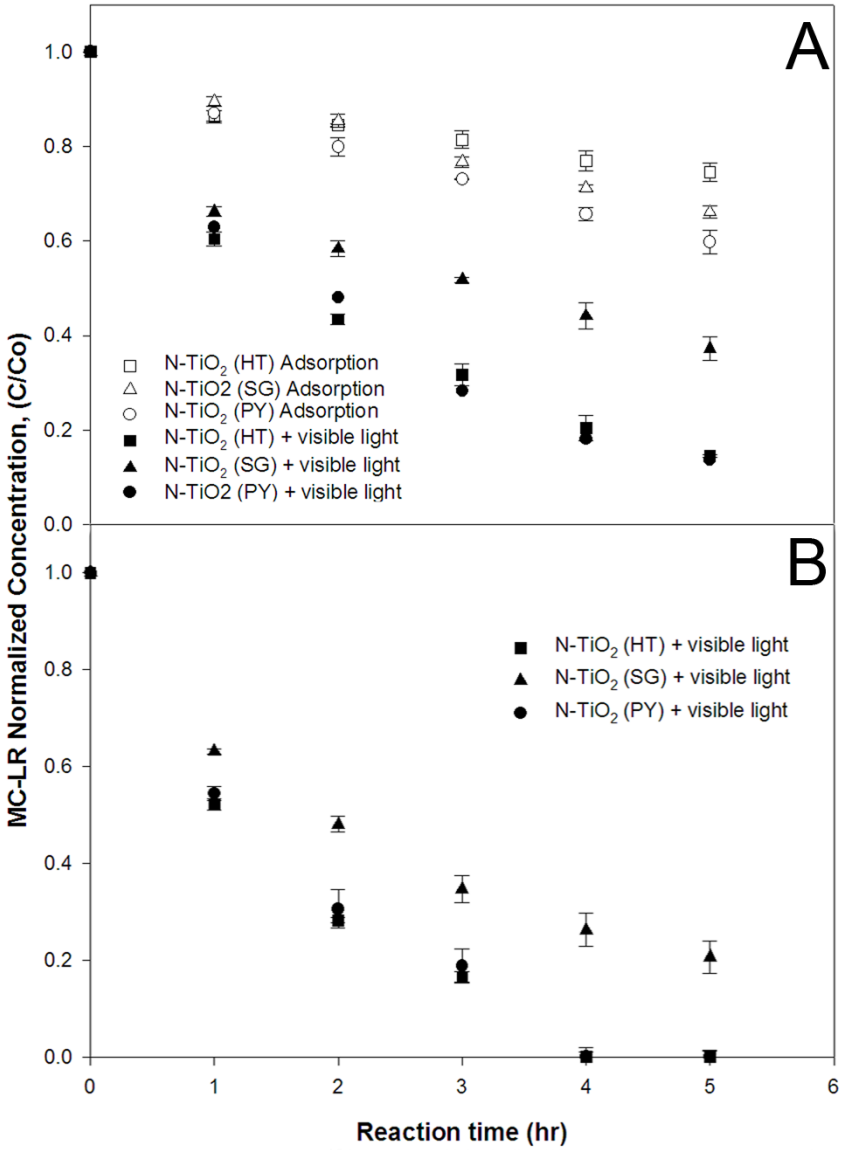

Figure 4: MC-LR photocatalytic degradation under visible light (λ>420 nm) with three N-TiO_2 photocatalysts. Conditions: Initial MC-LR concentration 600 µg/L, pH 3.0, A) N-TiO_2.loading: 0.5 g/L. B) N-TiO_2. loading: 1 g/L. In panel A evaluation of adsorption in dark conditions is also reported.

4 Conclusions

In this study, three differently prepared N-TiO_2 materials were synthesized and compared in order to establish some correlation between their main compositional and spectroscopic features and the photocatalytic activity under visible light. The main conclusions derived from the data here reported are as follows:

1) All materials contained nitrogen species of various types and showed high photocatalytic activity for the degradation of MC-LR with visible light irradiation.

2) The intensity of the optical absorption in the visible region was not correlated to the photocatalytic activity of the three N-TiO_2 samples. The pyrolitic sample (PY) in fact showed (Fig.1) a shift towards visible adsorption by far higher than that of the SG and HT samples but its photocatalic activity was similar to that of the HT sample.

3) The different preparation routes led to the formation of various impurities into the solids. In some cases these were weakly bound at the surface (HT and SG samples) while in the case of PY materials the impurities showed higher stability and can not be removed even at high temperature. On the basis of the photocatalytic data illustrated in this paper, the presence of such species was not detrimental for the photocatalytic activity of N-TiO_2 but actually contributed to a higher interaction with the target cyanotoxin; leading to a higher photocatalytic activity than the sol-gel samples.

4) The only species which absorbs visible light and which was common to all materials investigated here was the paramagnetic N_iO centre. This centre was individuated, in previous investigations of solids prepared via sol-gel [7] [8] [9], as the true visible light photoactive centre in such materials. Remarkably, this centre always forms, whatever the preparation route adopted, indicating that N containing compounds were introduced to the titanium matrix at high temperature. It is not easy to extract from the complex EPR spectra in Fig. 2 a direct evaluation of the amount of N_iO present in each material. At a first sight however, while the presence of this species is essential to photocatalytic activity, its abundance seems less determining.

5) A possible reason to explain the lower photocatalytic activity of sol-gel samples in MC-LR degradation, in comparison with the other two samples, is the presence of fluorine ions at the surface which derives from the use of NH_4F in the preparation. Fluorine ions induce a certain degree of hydrophobicity to the materials (monitored by TGA in terms of low desorption of water) which in the particular case of MC-LR could influence the contact of the molecules with the surface and the efficiency of the reaction. This point is currently under investigation in our labs.

Acknowledgement

This work is supported by CARIPLO Foundation through an Advanced Materials Grant 2009 and the Italian MIUR through the PRIN (Progetti di Ricerca di Interesse Nazionale) 2009. The TGA-FTIR measures have been obtained with the equipment acquired by the "G. Scansetti" Interdepartmental Centre for Studies on Asbestos and Other Toxic Particulates, thanks to a grant by the Compagnia di San Paolo, Torino, Italy. IC is recipient of a postdoctoral fellowship from the Compagnia di San Paolo, Italy. D. D. Dionysiou acknowledge support from the Cyprus Research Promotion Foundation through Desmi 2009-2010 which is co-funded by the Republic of Cyprus and the European Regional Development Fund of the EU under contract number NEA IPODOMI/STRATH/0308/09.

References

[1] M.A. Henderson, Surf. Sci. Rep. 66 (2011) 185-297.
[2] C. Di Valentin, E. Finazzi, G. Pacchioni, A. Selloni, S. Livraghi, M.C. Paganini, E. Giamello, Chem. Phys. 339 (2007) 44-56.
[3] A. M. Czoska, S. Livraghi, M. Chiesa, E. Giamello, E. Finazzi, C. Di Valentin, G. Pacchioni, S. Agnoli, G. Granozzi, J. Phys. Chem. C 112 (2008) 8951–8956.
[4] B. Neumann, P. Bogdanoff, H. Tributsch, S. Sakthivel, H. Kisch J. Phys. Chem. B 109 (2005) 16579-16586
[5] C. Han, M. Pelaez, V. Likodimos, A. G. Kontos, P. Falaras, K. O'Shea, D. D. Dionysiou, Appl. Catal. B: Environmental 107 (2011) 77– 87
[6] R. Asahi, T. Morikawa, T. Ohwaki, K. Aoki, Y. Taga, Science 293 (2001) 269-271.
[7] C. Di Valentin, G. Pacchioni, A. Selloni, S. Livraghi, E. Giamello, J. Phys. Chem. B 109 (2005) 11414-11419.
[8] S. Livraghi, M.C. Paganini, E. Giamello, A. Selloni, C. Di Valentin, G. Pacchioni, J. Am. Chem. Soc. 128 (2006) 15666-15671.
[9] F. Napoli, M. Chiesa,; S. Livraghi, E. Giamello, S. Agnoli, G. Granozzi, G. Pacchioni, C. Di Valentin.; Chem. Phys. Lett. 477 **(**2009) 135-138.
[10] S.Z. Chen, P.Y. Zhang, D.M. Zhuang, W.P. Zhu, Catal. Commun. 5 (2004) 677-680.
[11] Y. Nosaka, M. Matsushita, J. Nishino, A.Y. Nosaka, Sci. Thecnol. Adv. Mater. 6, 2005, 143-148.
[12] S. Livraghi, M. Chierotti, E. Giamello, G. Magnacca, M.C. Paganini, G. Cappelletti, C. Bianchi, J. Phys. Chem. C 112 (2008) 17244-17252.
[13] M. G. Antoniou, J. A. Shoemaker, A. A. de la Cruz, D. D. Dionysiou, Toxicon 51 (2008) 1103-1118
[14] H. Choi, M.G. Antoniou, M. Pelaez, A. A. De la Cruz, J. A. Shoemaker, D. D. Dionysiou, *Environ. Sci. Technol.* 41 (2007) 7530-7535
[15] M. Pelaez, A. A. de la Cruz, E. Stathatos, P. Falaras, D. D. Dionysiou, *Catalysis Today* 144 (2009) 19-25
[16] M. Pelaez, P. Falaras, V. Likodimos, A.G. Kontos, A.A. de la Cruz, K. O'Shea, D.D. Dionysiou, *Appl. Catal., B* 99 (2010) 378–387
[17] D. Graham, H. Kisch, L. A. Lawton, P. K. J. Robertson. *Chemosphere* 78 (2010) 1182-1185
[18] C. Di Valentin, E. Finazzi, G. Pacchioni, A. Selloni, S. Livraghi, A.M. Czoska, M.C. Paganini, E. Giamello, Chem. Mater. 20 (2008) 3706-3714.
[19] [M. Pelaez, A.A. de la Cruz, K. O'Shea, P. Falaras, D.D. Dionysiou, *Water Research* 45 (2011) 3787-3796].
[20] S. Livraghi, M.C. Paganini, M. Chiesa, E. Giamello, Res. Chem. Intermed. 33, (2007), 739–747.
[21] Y. Xie, Y. Li, X. Zhao, J. Mol. Catal. A: Chemical 277 (2007) 119–126.
[22] G. Martra, Appl. Catal. A: General 200 (2000) 275-285.
[23] M. Minella, M. G. Faga, V. Maurino, C. Minero, E. Pelizzetti, S. Coluccia, G. Martra, Langmuir 26 (2010) 2521–2527.
[24] G. Cerrato, G. Magnacca, C. Morterra, J. Montero, J. A. Anderson, J. Phys. Chem. C 113 (2009**)** 20401–20410.
[25] S. Usseglio, A. Damin, D. Scarano, S. Bordiga, A. Zecchina, C. Lamberti, J. Am. Chem. Soc. 129 (2007) 2822-2828.
[26] J. P. Chen, K. Isa, J. Mass Spectrom. Soc. Jpn. 46 (1998) 299-303.
[27] A. M. Bernhard, D. Peitz, M. Elsener, A. Wokaun, O. Kröcher, Appl. Catal. B: Environmental 115– 116 (2012) 129– 137
[28] D. Mitoraj, H. Kisch, Angew. Chem. Int. Ed. 47 (2008) 9975 –9978.
[29] X. Wang, K. Maeda, A. Thomas, K. Takanabe, G. Xin, J. M. Carlsson, K. Domen, M. Antonietti, Nature Materials 8 (2009) 76-80.

[30] F. Solymosi T. Bansagi, J. Catal. 202 (2001) 205–206.
[31] M. Janovska, Z. Bastl, Infrared Phys. Technol. 37 (1996) 727–731.
[32] S-i. Aoqui, T. Ohshima, T. Ikegami, K. Ebihara, Sci. Technol. Adv. Mat. 2 (2001) 533-537.
[33] G. Socrates, Infrared and Raman characteristic Group frequencies, Wiley, 3° edition 2001